Biosensors and Bioelectronics 45 (2013) 252–259

Contents lists available at SciVerse ScienceDirect

Biosensors and Bioelectronics

journal homepage: www.elsevier.com/locate/bios

Biomolecular recognition with a sensitivity-enhanced nanowire transistor biosensor

Bor-Ran Li [a,b], Chien-Wei Chen [b], Wan-Ling Yang [a], Ti-Yu Lin [a,c], Chien-Yuan Pan [c,d], Yit-Tsong Chen [a,b,*]

[a] Department of Chemistry, National Taiwan University, No. 1, Section 4, Roosevelt Road, Taipei 106, Taiwan
[b] Institute of Atomic and Molecular Sciences, Academia Sinica, P.O. Box 23-166, Taipei 106, Taiwan
[c] Institute of Zoology, National Taiwan University, No. 1, Section 4, Roosevelt Road, Taipei 106, Taiwan
[d] Department of Life Science, National Taiwan University, No. 1, Section 4, Roosevelt Road, Taipei 106, Taiwan

ARTICLE INFO

Article history:
Received 2 November 2012
Received in revised form
5 February 2013
Accepted 6 February 2013
Available online 17 February 2013

Keywords:
Nanowire biosensor
Field-effect transistor
Selective surface modification
Biotin
Avidin
Dopamine
PC12 cell

ABSTRACT

In applications of silicon nanowire field-effect transistors (SiNW-FETs) as biosensors, the SiNW-FETs conventionally are all area modified (AAM), with receptors covering not only the minute SiNW surface area but also the relatively large surrounding substrate area. In this study, using a bottom-up technique, we successfully fabricated selective surface modified (SSM) SiNW-FETs with the receptors on the SiNW sensing surface only. In this approach, the strategy was to modify the SiNWs with a chemical linker of 3-aminopropyltrimethoxysilane (APTMS) prior to photolithographic fabrication of the device. The APTMS molecules modifying the SiNWs survived the harsh photolithographic processes, including coating with photoresist, washing with organic solvent, and thermal annealing. These SSM SiNW-FETs also exhibited desirable electrical characteristics such as ohmic contact and high transconductance. Using the biotin–avidin binding system, we showed that the faster response time and smaller sample requirements of the SSM SiNW-FETs, relative to the conventional AAM SiNW-FETs, clearly show that restricting the surface modification of the SiNW-FETs substantially improves their detection sensitivity. Detection with a SSM boronic acid-modified SiNW-FET of the dopamine released under high-K^+ buffer stimulation from living PC12 cells also demonstrates that SiNW-FETs can serve as highly sensitive biosensors for biomedical diagnosis. In binding affinity measurements with SiNW-FETs, the dissociation constants (K_d) of the biotin–avidin and dopamine–boronic acid complexes were determined to be 15 ± 1 fM and 33 ± 8 fM, respectively.

© 2013 Elsevier B.V. All rights reserved.

1. Introduction

In the past decade, nanoscale field-effect transistors (FETs) have attracted great attention because of their potential as ultra-sensitive sensors for biomolecular detection (Chen et al., 2011; Cui et al., 2001; Liu et al., 2012; Stern et al., 2007a; Tans et al., 1998). In particular, the development of silicon nanowire FETs (SiNW-FETs), fabricated by both "bottom-up" (Lin et al., 2010; Patolsky et al., 2006) and "top-down" (Lin et al., 2009; Stern et al., 2007a) techniques, can take advantage of the processing techniques and mature fabrication methods of the silicon industry. To date, SiNW-FETs have been extensively employed for highly sensitive, label-free, and real-time detection of proteins (Lin et al., 2010; Wang et al., 2007), DNA (Hahm and Lieber, 2004), RNA (Zhang et al., 2009), cancer markers (Zheng et al., 2005), viruses (Chiang et al., 2012; Patolsky et al., 2004), and other species (Chen et al., 2011; Lieber, 2011).

Because SiNWs are normally covered with a thin silica sheath, from oxidation of their surfaces upon exposure to air, such SiNWs

Abbreviations: AAM, all area modified; AFM, atomic force microscopy; APTMS, 3-aminopropyltrimethoxysilane; biotin–HPDP, N-(6-(biotinamido)hexyl)-3′-(2′-pyridyldithio)-propionamide; BA/SiNW-FET, boronic acid modified SiNW-FET; CNT-FET, carbon nanotube field-effect transistor; CPBA, 4-carboxyphenylboronic acid; CVD, chemical vapor deposition; C_{avidin}, concentration of avidin; $C_{dopamine}$, concentration of dopamine; C_{K^+}, concentration of potassium ion; DI, deionized; DMSO, dimethyl sulfoxide; ESCA, electron spectroscopy for chemical analysis; EDC, 1-ethyl-3-(3-dimethylaminopropyl)carbodiimide hydrochloride; FET, field-effect transistor; I_{sd}, source–drain current; K_d, dissociation constant; KPFM, Kelvin probe force microscopy; MBS, 3-maleimidobenzoic acid N-hydroxy succinimide ester; NHS, N-hydroxysuccinimide; PBS, phosphate buffered saline; PDMS, polydimethylsiloxane; p*I*, isoelectric point; SSM, selective surface modification; SiNW-FET, silicon nanowire field-effect transistor; V_g, gate voltage; V_g^{cal}, calibrated response; V_{sd}, source–drain voltage

* Corresponding author at: Department of Chemistry, National Taiwan University, No. 1, Section 4, Roosevelt Road, Taipei 106, Taiwan.
Tel.: +886 2 3366 8198; fax: +886 2 3366 8671.
E-mail address: ytcchem@ntu.edu.tw (Y.-T. Chen).

0956-5663/$ - see front matter © 2013 Elsevier B.V. All rights reserved.
http://dx.doi.org/10.1016/j.bios.2013.02.009

have no chemical specificity toward particular analytes. Fortunately, SiNW-FET surfaces can be modified with selected receptors that subsequently allow them to achieve selectivity and nano- to femtomolar detection limits for specific target molecules (Cui et al., 2001; Pui et al., 2011; Pui et al., 2009). One economical, efficient, and commonly used SiNW-FET surface-modification method is to use a chemical linker, e.g., 3-aminopropyltrimethoxysilane (APTMS), which immobilizes the receptor and anchors to the silica sheath of the SiNW at opposite ends of the linker. However, the silica sheath on the SiNW surface is no different from the oxidized layer of a silicon wafer, which is usually used as a substrate for fabrication of SiNW-FET devices. Upon surface modification, receptor molecules are immobilized over the entire silica surface, covering not only the minute SiNW surface but also the relatively large surrounding substrate area. These types of SiNW-FET devices, which have all area modification (AAM), are denoted AAM SiNW-FETs (as illustrated in Schemes 1 and 2). The ratio of the surface area of the SiNW to the area of the surrounding substrate reflects the relative probabilities of these two surfaces coming into contact with an analyte molecule. In biosensing measurements using an AAM SiNW-FET coupled with a microfluidic channel (dimensions on the order of micrometers) to guide the flow of the sample solution, the ratio of the surface areas of the SiNW and the surrounding substrate is very small. This small ratio is undesirable because a large proportion of target molecules are likely to be captured by the receptors immobilized on the surrounding substrate before arriving at the actual SiNW-FET device; the large proportion of captured molecules consequently jeopardizes the detection sensitivity of the AAM SiNW-FET (Schemes 1 and 2).

SiNW-FETs that have selective surface modification (SSM), with receptors modifying only the SiNW surface without contaminating the surrounding substrate, are referred to as SSM SiNW-FETs (Schemes 1 and 2). Several approaches that have been used to reduce the modification by receptors on the non-sensing area include photolithography (Stern et al., 2007b), microcontact printing (Renault et al., 2002), electrostatic attraction (Naujoks

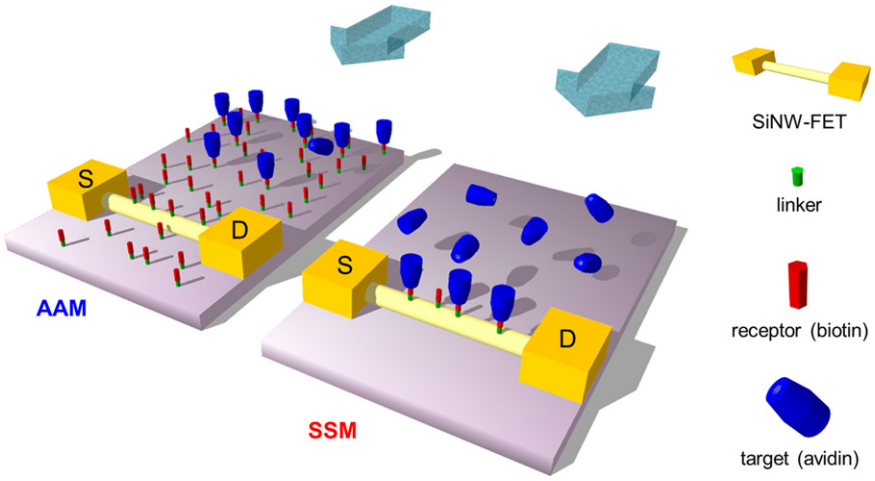

Scheme 1. An illustration depicting the binding competition involved in biomolecular detection by AAM or SSM SiNW-FET.

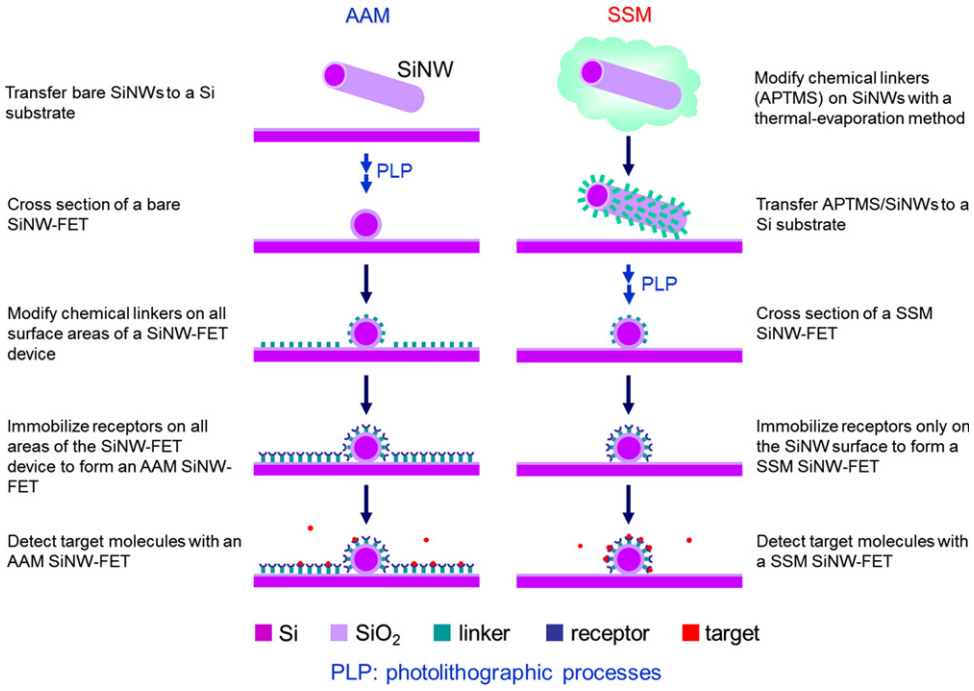

Scheme 2. Schematic representations of the preparation, fabrication, and biosensing of AAM and SSM SiNW-FETs.

and Stemmer, 2003), dip-pen nanolithography (Piner et al., 1999), localized Joule heating (Park et al., 2007), and incomplete chemical etching methods (Masood et al., 2010). Despite the localized surface modification, these methods are more suited to a silicon on insulator (SOI)-based top-down approach and require skilled labor.

Compared with top-down techniques, bottom-up methods have advantages in synthesizing SiNWs with high crystallinity, designated dopant density, a thin silica sheath, and easily controlled diameters with a cost-effective preparation (Chen et al., 2011). With the bottom-up approach, 2D mesh FETs for crossbar memory switches (Chen et al., 2006) and a 3D FET nanoprobe for recording intracellular signals (Tian et al., 2010) have recently been successfully fabricated. These FET structures may lead to device fabrication strategies that are not possible with top-down methods (Lieber, 2011). In this study, the strategy is to modify the SiNWs with APTMS (forming APTMS/SiNWs) prior to photolithographic fabrication of SSM APTMS/SiNW-FET devices. Subsequently, receptors are anchored to the SSM APTMS/SiNW-FET, transforming it into a SSM receptor/SiNW-FET that detects target molecules.

In tests, we first applied the biotin–avidin binding system to demonstrate the increased detection sensitivity of SSM SiNW-FETs compared with AAM SiNW-FETs. Furthermore, we employed a SSM boronic acid-modified SiNW-FET (BA/SiNW-FET) to detect the trace amount of dopamine released under high-K^+ buffer stimulation from living PC12 cells. This ultrasensitive molecular recognition and cellular detection allows SSM SiNW-FETs to act as powerful biosensors in medicine and the life sciences. For instance, neurons and adrenal glands synthesize catecholamines for neurotransmission and physiological functions; abnormal catecholamine concentrations in urine and blood are indicators of neuroblastoma and pheochromocytoma (Poirier et al., 2012; Strenger et al., 2007). Traditional electrochemical methods with a detection sensitivity of $\sim 10^{-8}$ M have been applied to detect catecholamines (Hu et al., 2008) and the dopamine secreted from chromaffin or PC12 cells in single exocytotic events (Kim et al., 2013). However, a diagnostic tool capable of sensing 10^{-13} M catecholamine is often required to detect the minute amount of catecholamines in biological samples (Davis et al., 1991). In this study, we will show that the SSM BA/SiNW-FET is able to detect 10^{-15} M dopamine and that this detection limit is promising for use of SSM BA/SiNW-FET in diagnosing the low dopamine levels normally present in urine or blood samples.

2. Materials and methods

2.1. Materials and reagents

Deionized (DI) water ($> 18\ M\Omega \cdot cm$) obtained from a purification system (Millipore Synergy) was used throughout the experiments. The phosphate buffered saline (1 × PBS) consisted of 137 mM NaCl, 2.7 mM KCl, 10 mM Na_2HPO_4, and 2 mM KH_2PO_4 in NaOH at pH 7.4. Commercially purchased chemical reagents and biological samples are listed in Section S1 of the Supplementary data

2.2. SiNW synthesis and device fabrication

Synthesis of the single-crystalline boron-doped SiNWs (Si:B=4000:1) was catalyzed by 20 nm gold nanoparticles in a chemical vapor deposition (CVD) reaction with the vapor–liquid–solid (VLS) growth mechanism (Yang et al., 2004). The quality of the as-synthesized *p*-type SiNWs was examined by high-resolution transmission electron microscopy (HR-TEM) and electron diffraction (ED) (JEM-2000FXΠ), as shown in Fig. S1 of the Supplementary data. The SiNW-FET devices were fabricated following standard photolithographic procedures (Patolsky et al., 2006). Details of the SiNW synthesis and device fabrication are given in Sections S2 and S3 of the Supplementary data.

2.3. Surface modification

2.3.1. Modification of APTMS on SiNW-FETs

SSM APTMS/SiNW-FETs were produced by surface modification of the SiNWs with thermally vaporized APTMS (Fig. S2) prior to photolithographic device fabrication. The detailed protocol for preparing SSM APTMS/SiNWs is described in Section S4 of the Supplementary data. Electron spectroscopy for chemical analysis (ESCA) of the prepared APTMS/SiNWs is shown in Fig. S3.

In the preparation of conventional AAM APTMS/SiNW-FETs, APTMS was immobilized on the silica surface of the entire device chip through solution-phase modification, of which technical details can be found in previous publications (Chang et al., 2012; Chiang et al., 2012; Lin et al., 2009, 2010; Tsai et al., 2011).

2.3.2. Immobilization of biotin

To anchor biotin on either the SSM APTMS/SiNW-FETs or the AAM APTMS/SiNW-FETs, the chip containing APTMS/SiNW-FETs was immersed for 30 min in a 1:9 (v/v) solution of DMSO and 1 × PBS containing 1 mM MBS. After MBS reacted with APTMS through the formation of an amide bond, the chip was rinsed with DI water, blown dry with N_2 gas, and immersed for 1 h in a 1:9 (v/v) solution of DMSO and 1 × PBS containing 5 mM biotin–HPDP and 100 mM dithiothreitol. After the sulfhydryl group of biotin–HPDP reacted with the maleimide group of MBS to immobilize the biotin on the APTMS/SiNW-FETs (forming biotin/SiNW-FETs), the chip was washed again with 1 × PBS and DI water, and finally, blown dry with N_2 gas (Lin et al., 2008; Nakajima and Ikada, 1995).

2.3.3. Immobilization of boronic acid

Modification of APTMS/SiNW-FETs with boronic acid to form BA/SiNW-FETs was carried out by coupling the amino group of APTMS with CPBA (5 mM) with the activators EDC (1 mM) and NHS (1 mM) in 1 × PBS for 10 min. The chip was subsequently washed with 1 × PBS and DI water and blown dry with N_2 gas (Lin et al., 2008).

2.4. Surface potential

The surface potential of an APTMS/SiNW was scanned by Kelvin probe force microscopy (KPFM) in a Digital Instruments/Veeco Bioscope SZ atomic force microscope (AFM) with a Nanoscope IVa controller under ambient conditions (moisture at $55 \pm 2\%$). The operational details of the KPFM measurements can be found in our previous publication (Tsai et al., 2011) and in Section S5 of the Supplementary data.

2.5. Electrical measurements

For electrical measurements of the SiNW-FETs, a digital multimeter (Keithley 6487), a lock-in amplifier (Stanford Research System, SR830), and a data acquisition system (National Instruments, DAQ BNC-2110) were employed. The experimental setup, reproducibility of the electrical measurements, and the operational details are shown in Figs. S4, S5, and Section S6 of the Supplementary data, respectively.

2.6. Preparation and stimulation of PC12 cells

The PC12 cell line was cultured in Dulbecco's modified Eagle's medium at 37 °C in an atmosphere containing 10% CO_2, and the medium was changed every other day. The suspended PC12 cells were stimulated with different concentrations of K^+ buffer for 10 min. The cells were then centrifuged, and the supernatant was collected for measurement. Details of the preparation and stimulation of PC12 cells are described in Section S7 of the Supplementary data

3. Results and discussion

3.1. Characterizations of the as-fabricated SiNW-FETs

Successful production of SSM APTMS/SiNW-FETs depends heavily on the APTMS molecules (which modify the SiNW surface) surviving a series of harsh fabrication processes, involving coating with photoresist, incubating with organic solvent, and annealing at 380 °C for 2 min in forming gas. Avoiding wire aggregation in the APTMS/SiNWs is also crucial for subsequent device fabrication. As shown in Fig. 1A, the modification with APTMS via thermal evaporation ((i) and (ii)) enabled the production of a large number of well-separated APTMS/SiNWs, in sharp contrast to the aggregated APTMS/SiNWs that resulted from solution-phase modification ((iii) and (iv)).

In Fig. 1B, panels (i) and (iii) show AFM images of an APTMS/SiNW and a bare SiNW, respectively, on a Si substrate, and panels (ii) and (iv) display the corresponding KPFM images. Consistent with previous reports, the surface potential of the APTMS/SiNW, in (ii), is higher than that of the bare SiNW, in (iv), by 38 ± 3 mV (from five measurements) (Gangopadhyay and De, 2000; Zou et al., 2008). The approximately constant surface potential along the APTMS/SiNW indicates the uniformity of the surface modification. An APTMS/Si substrate was also examined by ESCA after coating with photoresist, washing with organic solvent, and thermal annealing (Figs. 1C and S3). As shown in Fig. 1C, the N_{1s} signal at 401 eV in the ESCA spectrum corresponds to the APTMS molecules that survived the photolithographic process (80 ± 5% from three measurements (red) compared to 100% for the pristine APTMS/Si substrate (blue) and 0% for the bare Si substrate (black)). The high preservation of APTMS during the harsh photolithographic processing indicates that the fabrication of SSM APTMS/SiNW-FETs with this bottom-up technique has potential.

In Fig. 1D, the successfully modified SSM APTMS/SiNW-FET and AAM APTMS/SiNW-FET were further analyzed by their source–drain current as a function of the gate voltage (I_{sd}–V_g). For both devices, a high transconductance of $\sim 5.0 \pm 0.3$ μS was measured in 0.01 × PBS. In the inset, an ohmic contact in the as-fabricated SSM APTMS/SiNW-FET is indicated by the linear relation between the source–drain current and the bias voltage (I_{sd}–V_{sd}) plot; this result is comparable to previous results for AAM SiNW-FETs (Cui et al., 2001). Fig. S6 shows the electrical conductance of SSM APTMS/SiNW-FET in buffer solutions with various pH values, similar to previous results for an AAM APTMS/SiNW-FET (Cui et al., 2001); the conductance remains constant at each given pH and increases stepwise with pH from 5.0 to 8.5. At low pH, the NH_2 group is protonated to form NH_3^+ (Vezenov et al., 1997) and acts as a positive gate, which depletes hole carriers in the *p*-type SiNW and decreases the conductance. At high pH, SiOH is deprotonated to form SiO^-, which correspondingly causes an increase in conductance. The observed pH

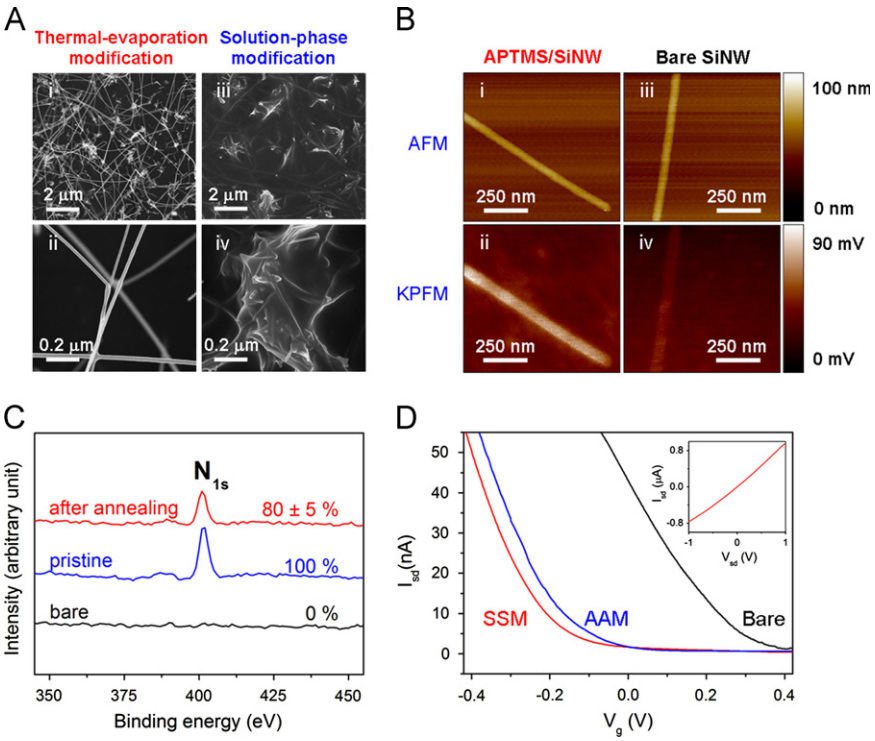

Fig. 1. The APTMS modification of SiNW-FETs. (A) Scanning electron microscopy (SEM) images at different magnifications of APTMS/SiNWs. (i) and (ii) are the APTMS/SiNWs prepared by thermal-evaporation. (iii) and (iv) are APTMS/SiNWs prepared by solution-phase modification. (B) AFM (upper row) and KPFM (lower row) images of an APTMS/SiNW (left column) and a bare SiNW (right column). (C) ESCA spectra of a bare Si substrate (black), a pristine APTMS/Si substrate (blue), and an APTMS/Si substrate after the series of photolithographic and annealing processes required during device fabrication (red). (D) The I_{sd}–V_g curves (measured at V_{sd} = 30 mV) of a bare SiNW-FET (black), an AAM APTMS/SiNW-FET (blue), and a SSM APTMS/SiNW-FET (red) in 0.01 × PBS at pH 7.4. (For interpretation of the references to color in this figure legend, the reader is referred to the web version of this article.)

response over a wide range can be attributed to an approximately linear change in the total surface charge density (versus pH) because of the combined acid and base behavior of both surface groups. In bare SiNW-FETs (with only SiOH functionality), the conductance should be nearly constant at pH < 6 but grow exponentially at pH > 6 (Bolt, 1957; Cui et al., 2001). The observed threshold-voltage shift (shown in Fig. 1D relative to a bare SiNW-FET) and the sensitive pH responses (in Fig. S6) indicate that the surface of the as-fabricated SSM APTMS/SiNW-FET device was well functionalized with reactive amino groups.

3.2. Enhanced detection sensitivity

3.2.1. Detection of avidin with biotin/SiNW-FET

We chose the biotin–avidin binding system to be a model to compare the detection sensitivities of SSM and AAM SiNW-FETs by anchoring biotin to both devices to detect avidin (Fig. S4A). To avoid device-to-device variation in detection sensitivity (Ishikawa et al., 2009), in biosensing experiments with SiNW-FETs, the current change (ΔI_{sd}) in response to binding between the receptor and target was transformed to the corresponding change in gate-voltage change (termed the calibrated response and represented by ΔV_g^{cal}) with the I_{sd}–V_g transfer curve of the FET device used (as displayed in Fig. S7). In Fig. 2A, biotin/SiNW-FETs were used to detect 10 nM avidin (in 0.01× PBS) that flowed at 0.3 mL/hr through a polydimethylsiloxane (PDMS) microfluidic channel above the FET-devices. The upper right and left illustrations compare the real time detection by the AAM and SSM biotin/SiNW-FETs, respectively; the bottom panels show the differences in the response times for avidin detection (10 nM, 100 nM, and 1 μM) by SSM biotin/SiNW-FET (red traces) and AAM biotin/SiNW-FET (blue traces). The detection of avidin (pI=10.5) in 0.01× PBS at pH 7.4 with a p-type biotin/SiNW-FET causes a decrease in the electrical conductance because of a gating effect. Upon reaching the biotin–avidin binding equilibrium, the changes in V_g^{cal} from both the SSM and AAM devices are nearly identical, indicating that the binding sites of the SSM and AAM biotin/SiNW-FETs captured an approximately equal number of avidin molecules. However, at low sample concentrations (e.g., 100 and 10 nM), a much longer response time is required by the AAM biotin/SiNW-FET to reach equilibrium compared with the SSM biotin/SiNW-FET; this result clearly indicates the avidin-binding competition between the biotins immobilized on the SiNW and the surrounding substrate in the AAM device (upper illustrations in Fig. 2A and Schemes 1 and 2). Given the very small ratio of the surface areas of the SiNW and the surrounding substrate, a significant proportion of the avidin is captured by the biotins on the surrounding substrate before arriving at the binding sites on the SiNW, resulting in the longer response time (i.e., larger sample volume required) of the AAM biotin/SiNW-FET.

In addition, the SSM and AAM biotin/SiNW-FETs were compared by detecting a finite volume (5 μL) of an avidin solution (in 0.01× PBS) at various concentrations (C_{avidin}=1 fM–1 nM) (Fig. S4B). Figs. 2B and 2C show the I_{sd}–V_{sd} curves measured with AAM and SSM biotin/SiNW-FETs, respectively. The measured I_{sd} data at V_{sd} = −0.1 V were transformed to V_g^{cal} and are summarized in Fig. 2D as a function of C_{avidin}. Notably, although 5 μL of 1 fM avidin caused a sizable change of V_g^{cal} ~5 mV in the SSM biosensor, the response of the AAM sensor is negligible for the same sample solution. At 100 fM, a difference in V_g^{cal} of ~20 mV

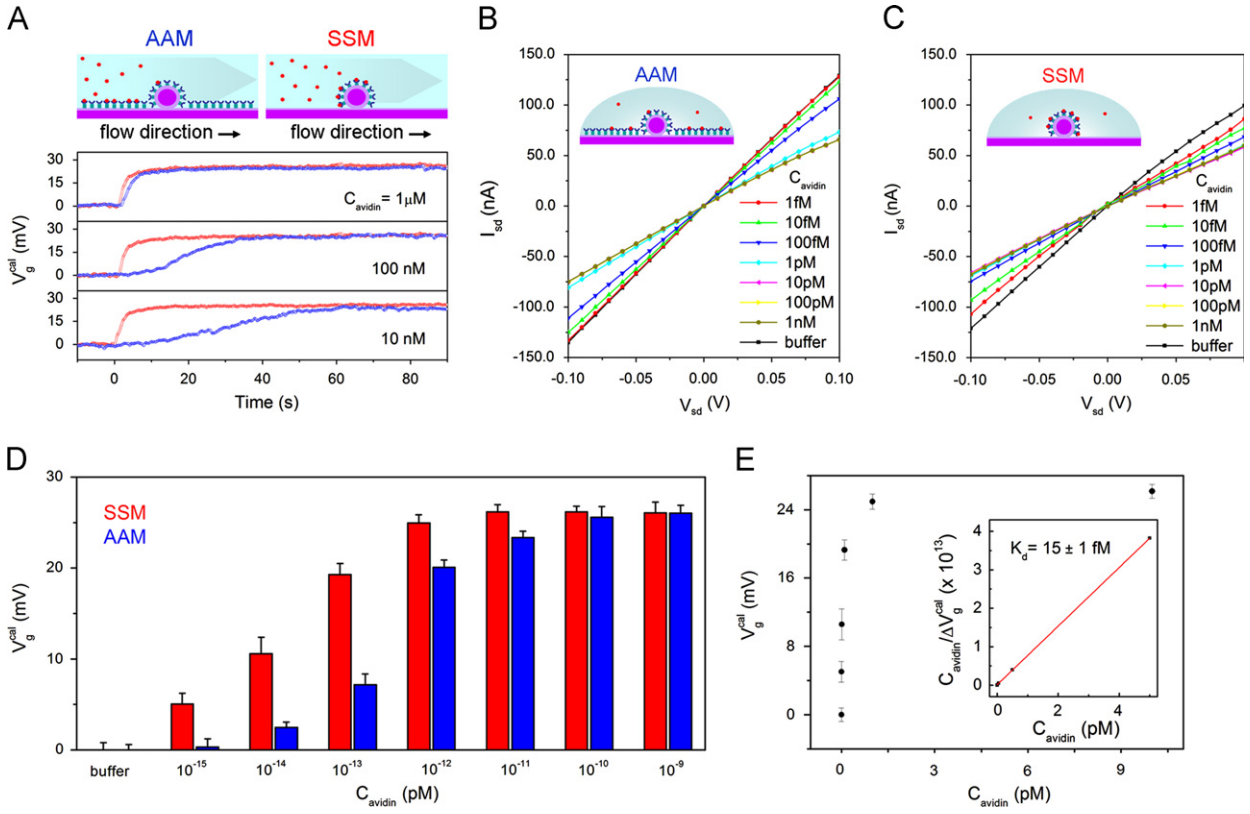

Fig. 2. Detection of avidin with SSM (AAM) biotin/SiNW-FET. (A) Real time recordings of V_g^{cal} while avidin at 10 nM, 100 nM, and 1 μM, was perfused onto the SSM biotin/SiNW-FET (red traces) and the AAM biotin/SiNW-FET (blue traces). (B) and (C) show the I_{sd}–V_{sd} curves measured by the AAM and SSM biotin/SiNW-FETs, respectively, for detection of 5 μL avidin at C_{avidin}=1 fM–1 nM. (D) A column plot of V_g^{cal} at different C_{avidin}. The V_g^{cal} values were transformed from the measured I_{sd} at V_{sd} = −0.1 V in (B) and (C) with the I_{sd}–V_g transfer curve of the AAM (blue) and SSM (red) biotin-SiNW-FETs. The error bars present the standard deviations of three measurements. (E) A plot of V_g^{cal} as a function C_{avidin} is summarized from the data in (D) measured by SSM biotin/SiNW-FET. The inset shows a least-squares fit (Eq. (1)) of the measured $C_{avidin}/\Delta V_g^{cal}$ as a function of C_{avidin}. (For interpretation of the references to color in this figure legend, the reader is referred to the web version of this article.)

(SSM) vs. ~8 mV (AAM) is observed. Moreover, a 5 μL drop of 1 pM avidin almost saturated the SSM biotin/SiNW-FET; in contrast, the AAM biotin/SiNW-FET did not saturate until $C_{avidin} \geq 100$ pM. These results demonstrate that the SSM system is more sensitive than the AAM to trace detection in a tiny sample volume.

The dissociation constant (K_d) of the biotin–avidin complex can be determined by a least-squares fit of the $V_g^{cal}-C_{avidin}$ data (in Fig. 2D) to the Langmuir adsorption isotherm model (Chang et al., 2012; Ohno et al., 2009):

$$\frac{C_{avidin}}{\Delta V_g^{cal}} = \frac{1}{\Delta V_{g,\,max}^{cal}} C_{avidin} + \frac{1}{\Delta V_{g,\,max}^{cal}} K_d \quad (1)$$

where the relative ΔV_g^{cal} is defined as $\Delta V_g^{cal}(\%) = V_g^{cal} - V_{g,0}^{cal}/V_{g,0}^{cal} \times 100(\%)$, $V_{g,0}^{cal}$ is the calibrated response at $C_{avidin}=0$ that induces no detectable signal, and $V_{g,max}^{cal}$ is the saturated calibrated response at high C_{avidin}. As shown in Fig. 2E, a least-squares fit (Eq. (1)) of the $V_g^{cal}-C_{avidin}$ data measured with the SSM biotin/SiNW-FET (Fig. 2D) yields $K_d = 15 \pm 1$ fM for the biotin–avidin complex; this result is consistent with the K_d value obtained in previous studies (Laitinen et al. 2006). In comparison, a least-squares fit (Eq. (1)) of the $V_g^{cal}-C_{avidin}$ data measured with the AAM biotin/SiNW-FET (Fig. 2D) gives $K_d = 324 \pm 173$ fM; the considerable uncertainty and much larger K_d (by ~20 times) indicates inaccuracy compared with the SSM biotin/SiNW-FET. This result is observed because the number of avidins that could bind to the AAM biotin/SiNW-FET is too low to reach the biotin–avidin equilibrium, especially at very low C_{avidin}. As indicated in Fig. 2D, the smaller V_g^{cal} measured by the AAM system at $C_{avidin} \leq 10$ pM (relative to the SSM system) arises because in the AAM biotin/SiNW-FET measurements, part of the avidins were captured on the surrounding substrate before arriving at the binding sites on the SiNW, resulting in deficient avidins to reach a genuine biotin–avidin equilibrium. This deterioration in accuracy is enhanced as C_{avidin} decreases. Consequently, the association constant ($K_a = 1/K_d$) is underestimated by fitting the incomplete V_g^{cal} vs. C_{avidin} data for the AAM biotin/SiNW-FET to Eq. (1), leading to an overcalculated K_d of 324 ± 173 fM and a poor standard deviation.

3.2.2. Detection of dopamine released from PC12 cells

As nanoscale biosensors for molecular recognition, SiNW-FETs (and carbon nanotube (CNT)-FETs) have been successfully used to detect proteins, DNA/RNA, viruses, bacteria, mammalian cancer cells, and so on. However, most biomolecular analytes studied to date are large in size, with high molecular weights, and carry a large charge, which can exert a strong electric field and facilitate sensitive detections by FETs. It is comparatively challenging for FET-based biosensors to recognize weakly charged small molecules. To date, only a few small molecules have been studied with SiNW-FETs/CNT-FETs, e.g., label-free detection of adenosine-5′-triphosphate (Wang et al., 2005) and glutamate (Lee et al., 2009) and charge-enhancer assisted detection of adenosine (Zayats et al., 2006), cocaine (Sharon et al., 2009), and glucose (Cella et al. 2010).

In this study, we also detected dopamine (pI=8.93) (Sedeh et al., 1993), released from live PC12 cells by high-K^+ stimulation with SSM and AAM BA/SiNW-FETs (Fig. S4B) through the binding of BA with the diol group of dopamine (Nakajima and Ikada, 1995). Before the cellular experiments, a standard calibration curve was established by testing various concentrations of dopamine ($C_{dopamine}$=1 fM–100 pM) with BA/SiNW-FETs. The $I_{sd}-V_{sd}$ curves measured with a SSM BA/SiNW-FET are displayed in Fig. 3A with the corresponding $V_g^{cal}-C_{dopamine}$ plot at $V_{sd}=-0.1$ V in Fig. 3B. The linear response of the SSM BA/SiNW-FET to $C_{dopamine}$ spans from 1 fM to ~1 pM. In the inset, $K_d = 33 \pm 8$ fM

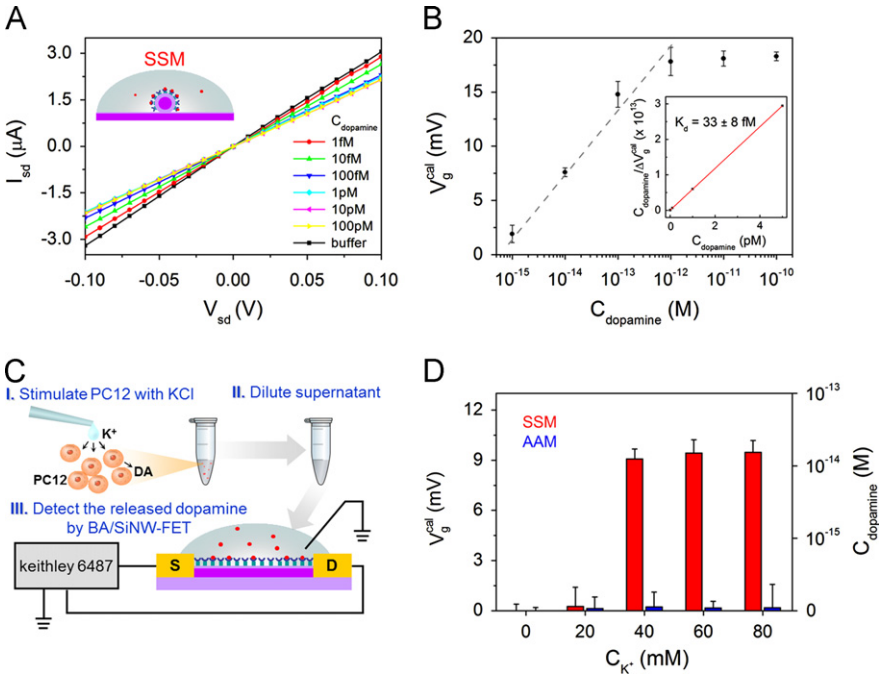

Fig. 3. Detection of dopamine released from PC12 cells. (A) The $I_{sd}-V_{sd}$ curves were measured with a SSM BA/SiNW-FET at $C_{dopamine}$=1 fM–100 pM. (B) The $V_g^{cal}-C_{dopamine}$ plot is transformed from the measured I_{sd} at $V_{sd}=-0.1$ V in (A). The dashed line marks the linear range for dopamine detection. The inset shows a least-squares fit (Eq. (1)) of the measured $C_{dopamine}/\Delta V_g^{cal}$ vs. $C_{dopamine}$. (C) An illustration of the experimental design for PC12 cells stimulation. PC12 cells were stimulated with high-K^+ buffer (I); after centrifuging the cells, the supernatant was diluted (II) and applied to a BA/SiNW-FET for V_g^{cal} measurement (III). (D) The V_g^{cal} values were measured from samples collected from PC12 cells stimulated with various K^+ concentrations. The V_g^{cal} values (left ordinate) measured with SSM (red) and AAM (blue) BA/SiNW-FETs were converted to the concentration of dopamine in the supernatant (right ordinate) according to the calibration curve shown in (B). (For interpretation of the references to color in this figure legend, the reader is referred to the web version of this article.)

for the dopamine–boronic acid complex is obtained by fitting the $V_g^{cal}-C_{dopamine}$ (1 fM − 100 pM) data points to Eq. (1).

We then used SSM and AAM BA/SiNW-FETs to detect the dopamine released under high-K^+ stimulation from live PC12 cells. As illustrated schematically in Fig. 3C, the suspended, living PC12 cells were stimulated for 10 min with a buffer containing potassium chloride at $C_{K^+}=20$, 40, 60, and 80 mM. After stimulation, the PC12 cells were removed by centrifugation, and the supernatant was diluted 1000-fold in 0.01 × PBS. For each C_{K^+}, 5 μL of the diluted supernatant was dropped directly on the BA/SiNW-FET device to quantify the released dopamine. Fig. 3D summarizes the amount of dopamine released from the PC12 cells at different C_{K^+} measured by SSM (red) and AAM (blue) BA/SiNW-FETs. At $C_{K^+}=20$ mM, the released $C_{dopamine}$, measured by either SSM or AAM BA/SiNW-FET, is negligible and is not significantly different from that of PC12 cells without stimulation ($C_{K^+}=0$ mM). Nevertheless, prominent releases of dopamine ($C_{dopamine}>10$ fM) were detected with a SSM BA/SiNW-FET for $C_{K^+}\geq 40$ mM; this detection is in sharp contrast to the very weak signals detected by AAM BA/SiNW-FET for the same C_{K^+}. These distinctive results demonstrate that a SiNW-FET device with restricted-area modification (restricting modification solely to the sensing surface) has a substantially improved detection sensitivity and can be used as an ultrasensitive biosensor for molecular recognitions.

Dopamine, a neurotransmitter in the central nervous system and a hormone secreted by adrenal medulla and excreted via urine, has a number of important physiological roles in the bodies of animals. The urinary dopamine level is a diagnostic indicator for neuroblastoma and pheochromocytoma (Poirier et al., 2012; Strenger et al., 2007). However, because of the low urinary dopamine level ($\sim 10^{-13}$ M) (Davis et al., 1991), it must usually be collected over a 24-hour period to ensure successful detection by traditional electrochemical methods with $\sim 10^{-8}$ M detection sensitivity. In contrast, the SSM SiNW-FET in this work was demonstrated to detect 10^{-15} M dopamine and has an advantage for the immediate biomedical diagnosis of dopamine present in urine or blood samples.

4. Conclusions

In summary, we have successfully fabricated SSM APTMS/SiNW-FETs using a bottom-up approach consisting of SiNW synthesis, APTMS modification, and lithographic fabrication. The fabricated SSM SiNW-FETs possess excellent electrode contact, modification efficiency, and transconductance qualities. Using the biotin–avidin binding system, we showed that a SSM SiNW-FET is a substantial improvement over an AAM SiNW-FET, due to superior detection sensitivity, faster response time, and smaller sample requirements, rendering the SSM SiNW-FET a highly sensitive biosensor for molecular recognitions. Detection with a SSM BA/SiNW-FET of the dopamine released under high-K^+ stimulation from living PC12 cells also shows that sensitive SSM SiNW-FETs can be utilized for immediate biomedical diagnosis. In the binding affinity measurements, the dissociation constants of the biotin–avidin and dopamine–boronic acid complexes were determined to be $K_d=15\pm 1$ fM and 33 ± 8 fM, respectively.

Acknowledgments

This work was partially supported by the National Science Council of Taiwan under Grants NSC 101-2627-M-002-004 and NSC 101-2627-M-002-013. B.-R. Li was supported by a postdoctoral fellowship from Academia Sinica. Technical support from NanoCore, the Core Facilities for Nanoscience and Nanotechnology at Academia Sinica, is acknowledged.

Appendix A. Supplementary materials

Supplementary data associated with this article can be found in the online version at http://dx.doi.org/10.1016/j.bios.2013.02.009.

References

Bolt, G.H., 1957. Journal of Physical Chemistry 61, 1166–1169.
Cella, L.N., Chen, W., Myung, N.V., Mulchandani, A., 2010. Journal of the American Chemical Society 132, 5024–5026.
Chang, K.S., Sun, C.J., Chiang, P.L., Chou, A.C., Lin, M.C., Liang, C., Hung, H.H., Yeh, Y.H., Chen, C.D., Pan, C.Y., Chen, Y.T., 2012. Biosensors and Bioelectronics 31, 137–143.
Chen, K.I., Li, B.R., Chen, Y.T., 2011. Nano Today 6, 131–154.
Chen, Z., Appenzeller, J., Lin, Y.M., Sippel-Oakley, J., Rinzler, A.G., Tang, J., Wind, S.J., Solomon, P.M., Avouris, P., 2006. Science 311, 1735.
Chiang, P.L., Chou, T.C., Wu, T.H., Li, C.C., Liao, C.D., Lin, J.Y., Tsai, M.H., Tsai, C.C., Sun, C.J., Wang, C.H., Fang, J.M., Chen, Y.T., 2012. Chemistry—An Asian Journal 7, 2073–2079.
Cui, Y., Wei, Q.Q., Park, H.K., Lieber, C.M., 2001. Science 293, 1289–1292.
Davis, K.L., Kahn, R.S., Ko, G., Davidson, M., 1991. American Journal of Psychiatry 148, 1474–1486.
Gangopadhyay, R., De, A., 2000. Chemistry of Materials 12, 2064.
Hahm, J., Lieber, C.M., 2004. Nano Letters 4, 51–54.
Hu, G.Z., Zhang, D.P., Wu, W.L., Yang, Z.S., 2008. Colloids and Surfaces B: Biointerfaces 62, 199–205.
Ishikawa, F.N., Curreli, M., Chang, H.K., Chen, P.C., Zhang, R., Cote, R.J., Thompson, M.E., Zhou, C.W., 2009. ACS Nano 3, 3969–3976.
Kim, B.N., Herbst, A.D., Kim, S.J., Minch, B.A., Lindau, M., 2013. Biosensors and Bioelectronics 41, 736–744.
Laitinen, O.H., Hytonen, V.P., Nordlund, H.R., Kulomaa, M.S., 2006. Cellular and Molecular Life Sciences 63, 2992–3017.
Lee, G.J., Lim, J.E., Park, J.H., Choi, S.K., Hong, S., Park, H.K., 2009. Current Applied Physics 9, S25–S28.
Lieber, C.M., 2011. MRS Bulletin 36, 1052–1063.
Lin, C.H., Hsiao, C.Y., Hung, C.H., Lo, Y.R., Lee, C.C., Su, C.J., Lin, H.C., Ko, F.H., Huang, T.Y., Yang, Y.S., 2008. Chemical Communications 44, 5749–5751.
Lin, S.P., Pan, C.Y., Tseng, K.C., Lin, M.C., Chen, C.D., Tsai, C.C., Yu, S.H., Sun, Y.C., Lin, T.W., Chen, Y.T., 2009. Nano Today 4, 235–243.
Lin, T.W., Hsieh, P.J., Lin, C.L., Fang, Y.Y., Yang, J.X., Tsai, C.C., Chiang, P.L., Pan, C.Y., Chen, Y.T., 2010. Proceedings of the National Academy of Sciences USA 107, 1047–1052.
Liu, Y.X., Dong, X.C., Chen, P., 2012. Chemical Society Reviews 41, 2283–2307.
Masood, M.N., Chen, S., Carlen, E.T., van den Berg, A., 2010. ACS Applied Materials and Interfaces 2, 3422–3428.
Nakajima, N., Ikada, Y., 1995. Bioconjugate Chemistry 6, 123–130.
Naujoks, N., Stemmer, A., 2003. Microelectronic Engineering 67-8, 736–741.
Ohno, Y., Maehashi, K., Yamashiro, Y., Matsumoto, K., 2009. Nano Letters 9, 3318–3322.
Park, I., Li, Z.Y., Pisano, A.P., Williams, R.S., 2007. Nano Letters 7, 3106–3111.
Patolsky, F., Zheng, G.F., Hayden, O., Lakadamyali, M., Zhuang, X.W., Lieber, C.M., 2004. Proceedings of the National Academy of Sciences USA 101, 14017–14022.
Patolsky, F., Zheng, G.F., Lieber, C.M., 2006. Nature Protocols 1, 1711–1724.
Piner, R.D., Zhu, J., Xu, F., Hong, S.H., Mirkin, C.A., 1999. Science 283, 661–663.
Poirier, E., Thauvette, D., Hogue, J.C., 2012. Journal of the American College of Surgeons 216, 340–346.
Pui, T.S., Agarwal, A., Ye, F., Huang, Y.X., Chen, P., 2011. Biosensors and Bioelectronics 26, 2746–2750.
Pui, T.S., Agarwal, A., Ye, F., Ton, Z.Q., Huang, Y.X., Chen, P., 2009. Nanoscale 1, 159–163.
Renault, J.P., Bernard, A., Juncker, D., Michel, B., Bosshard, H.R., Delamarche, E., 2002. Angewandte Chemie International Edition 41, 2320–2323.
Sedeh, I.F., Sjoberg, S., Ohman, L.O., 1993. Journal of Inorganic Biochemistry 50, 119–132.
Sharon, E., Freeman, R., Tel-Vered, R., Willner, I., 2009. Electroanalytical Chemistry 21, 1291–1296.
Stern, E., Klemic, J.F., Routenberg, D.A., Wyrembak, P.N., Turner-Evans, D.B., Hamilton, A.D., LaVan, D.A., Fahmy, T.M., Reed, M.A., 2007a. Nature 445, 519–522.
Stern, E., Wagner, R., Sigworth, F.J., Breaker, R., Fahmy, T.M., Reed, M.A., 2007b. Nano Letters 7, 3405–3409.
Strenger, V., Kerbl, R., Dornbusch, H.J., Ladenstein, R., Ambros, P.F., Ambros, I.M., Urban, C., 2007. Pediatric Blood and Cancer 48, 504–509.
Tans, S.J., Verschueren, A.R.M., Dekker, C., 1998. Nature 393, 49–52.

Tian, B.Z., Cohen-Karni, T., Qing, Q., Duan, X.J., Xie, P., Lieber, C.M., 2010. Science 329, 830–834.
Tsai, C.C., Chiang, P.L., Sun, C.J., Lin, T.W., Tsai, M.H., Chang, Y.C., Chen, Y.T., 2011. Nanotechnology 22, 135503.
Vezenov, D.V., Noy, A., Rozsnyai, L.F., Lieber, C.M., 1997. Journal of the American Chemical Society 119, 2006–2015.
Wang, C.W., Pan, C.Y., Wu, H.C., Shih, P.Y., Tsai, C.C., Liao, K.T., Lu, L.L., Hsieh, W.H., Chen, C.D., Chen, Y.T., 2007. Small 3, 1350–1355.
Wang, W.U., Chen, C., Lin, K.H., Fang, Y., Lieber, C.M., 2005. Proceedings of the National Academy of Sciences USA 102, 3208–3212.
Yang, Y.H., Wu, S.J., Chin, H.S., Lin, P.I., Chen, Y.T., 2004. Journal of Physical Chemistry B 108, 846–852.
Zayats, M., Huang, Y., Gill, R., Ma, C.A., Willner, I., 2006. Journal of the American Chemical Society 128, 13666–13667.
Zhang, G.J., Chua, J.H., Chee, R.E., Agarwal, A., Wong, S.M., 2009. Biosensors and Bioelectronics 24, 2504–2508.
Zheng, G.F., Patolsky, F., Cui, Y., Wang, W.U., Lieber, C.M., 2005. Nature Biotechnology 23, 1294–1301.
Zou, H., Wu, S.S., Shen, J., 2008. Chemical Reviews 108, 3893–3957.